Cámara F; Bellatreccia F; Della Ventura G; Gunter ME; Sebastiani M; Cavallo A. Kircherite, a new mineral of the cancrinite-sodalite group with a 36-layer stacking sequence: Occurrence and crystal structure.. AMERICAN MINERALOGIST. 97 pp: 1494-1504.
DOI: 10.2138/am.2012.4033

FIRST REVISION 20/03/2012

KIRCHERITE, A NEW MINERAL OF THE CANCRINITE - SODALITE GROUP WITH A 36-LAYER STACKING SEQUENCE: OCCURRENCE AND CRYSTAL STRUCTURE

Fernando Cámara[1]

[1] Dipartimento di Scienze della Terra, Università di Torino

Via Valperga Caluso 35, 10125 Torino, Italy

Fabio Bellatreccia[2], **Giancarlo Della Ventura**[2]

[2] Dipartimento Scienze Geologiche, Università Roma Tre,

Largo San Leonardo Murialdo 1, 00146 Rome, Italy

Mickey E. Gunter[3]

[3] Department of Geological Sciences, University of Idaho

Moscow Idaho, 83844-3022, USA

Marco Sebastiani[4]

[4] Dipartimento di Ingegneria Meccanica e Industriale, Università Roma Tre

Via della Vasca Navale 79, I-00146 Rome, Italy

Andrea Cavallo[5]

[5] Istituto Nazionale di Geofisica e Vulcanologia (I.N.G.V.),

Via di Vigna Murata 605, I-00143 Rome, Italy

Corresponding Author:

Fabio Bellatreccia. Dipartimento Scienze Geologiche, Università Roma Tre, Largo San Leonardo Murialdo 1, I-00146 Roma, Italy

e-mail: bellatre@uniroma3.it

Tel: +39-06 57 338 068

Fax: +39 06 57 338 201

Written on IBM compatible computer, MS Word text editor

ABSTRACT

This paper reports on the occurrence and the crystal structure of kircherite, a new member of the cancrinite-sodalite group of minerals from Valle Biachella, Sacrofano community (Rome, Latium, Italy). The mineral occurs in association with sodalite, biotite, iron oxides, titanite, fluorite and a pyrochlore-group mineral. The groundmass of the ejectum consists essentially of K-feldspar with subordinate plagioclase. Kircherite (3 mm as largest size) is observed within miarolitic cavities of the rock and typically occurs as parallel associations of hexagonal, thin, tabular colorless to light gray transparent crystals; it is non-pleochroic and uniaxial negative, with ω = 1.510(2) and ε = 1.502(2). D_{calc} is 2.457 g/cm^3. Kircherite is trigonal with *a* = 12.8770(7), *c* = 95.244(6) Å, *V* = 13677(1) Å^3, *Z* = 1. The structure has been refined in the trigonal space group *R*32, obtaining a R-value of 8.5% on 8131 reflections with I/σI>2. The strongest seven reflections in the X-ray powder pattern are [*d* in Å (I %) (*hkl*)]: 3.717 (100) (3 0 0), 2.648 (100) (2 1 28; 0 0 36), 3.232 (65) (2 1 19), 3.584 (60) (1 2 14), 3.604 (53) (1 0 25), 3.799 (52) (1 2 11), 3.220 (38) (2 2 0). The single-crystal FTIR spectrum rules out OH groups and shows the presence of H_2O and CO_2 molecules in the structural cages of the mineral. Chemical analysis gives (in wt%): SiO_2 32.05, Al_2O_3 27.13, FeO 0.07, K_2O 4.38, CaO 8.75, Na_2O 13.62, MgO 0.01, MnO 0.02, TiO_2 0.01, SO_3 12.87, Cl 0.35, F 0.05. The empirical formula calculated on the basis of Σ(Si+Al) = 216 apfu is:

$(Na_{89.09}Ca_{31.63}K_{18.85}Fe_{0.20}Mn_{0.06}Mg_{0.05}Ti_{0.03})_{\Sigma=139.91}[(Si_{108.13}Al_{107.87})_{\Sigma=216.00}O_{430.00}](SO_4)_{32.58}$ $Cl_{2.00}F_{0.53}\cdot 6.86H_2O$, which corresponds to the ideal formula $[Na_{90}Ca_{36}K_{18}]_{\Sigma=144}(Si_{108}Al_{108}O_{432})(SO_4)_{36}\cdot 6H_2O$.

The structure can be described as a stacking sequence of 36 layers of six-membered rings of tetrahedra along the *c* axis. The stacking sequence is ACABCABCABCACBCABCABCABCBABCABCABCAB…, where A, B and C represent the positions of the rings within the layers. This sequence gives rise to cancrinite, sodalite

and losod cages, alternating along *c*. Sulfate groups occur within the sodalite and losod cages associated by Na, K and Ca. H_2O groups occur within the cancrinite cages, bonded to Ca and Na cations. Anion groups (SO_4^{2-}) in sodalite cages show positional disorder, and so do consequently the extraframework cation sites to them related.

Keywords: New minerals, kircherite, ordered interstratified sodalites-cancrinite, crystal structure, IR spectroscopy, mechanical properties.

INTRODUCTION

The cancrinite group of feldspathoids includes several species structurally characterized by layers of six-membered rings of [SiO_4] and [AlO_4] tetrahedra stacked along the crystallographic *c* direction (hereafter 6mR $\perp$ [00.1]). The different stacking sequences give rise to different types of structural channels and cages (Bonaccorsi and Merlino 2005). These pores may host several anions and molecular groups, such as H_2O, Cl, $(CO_3)^{2-}$, $(SO_4)^{2-}$, $(S_2)^{-}$, $(S_3)^{-}$, $(PO_4)^{3-}$, $(C_2O_4)^{2-}$, CO_2 and extra-framework cations such as Na, K and Ca. The stacking sequence can be simple like …ABABAB… (where A and B are the positions in successive layers, using the notation of the closest-packed structures) as in cancrinite *sensu stricto*, or can be complex, leading to a variety of species for which sequences of 4, 6, 8, 10, 12, 14, 16, 28, 30, and 33 layers for the *c* translation have been described (for 4 to 16 see Table 2 in Bonaccorsi and Merlino 2005; 28 layers = sacrofanite: Bonaccorsi et al. 2012; 30 layers = biachellaite: Chukanov et al. 2008, Rastsvetaeva and Chukanov 2008; 33 layers = fantappièite: Cámara et al. 2010). Domains with 18 and 24 layer sequences were also observed by transmission electron microscopy (Rinaldi and Wenk 1979). An equal number of layers can also give rise to different sequences, like in marinellite (Bonaccorsi and Orlandi 2003) *vs* tounkite (Rozenberg et al. 2004), both structures having 12 layers sequences, or to different anion-cation population

of the cages. An example of this latter case is represented by afghanite and alloriite which, although having the same type of framework, differ in having Ca-Cl-Ca-Cl (Ballirano et al. 1997) or Na-H_2O-Na-H_2O (Chukanov et al. 2007; Rastsvetaeva et al. 2007) extraframework contents, respectively. Recently, carbobystrite has been described as having the same staking sequence of bystrite (ABAC) but having CO_3 and H_2O groups instead of S^{2-} as in bystrite (Khomyakov et al. 2010).

Kircherite was found -- and donated to us by Mr. L. Mattei (1947 - 2012), a distinguished amateur mineral collector -- within the miarolitic cavities of a holocrystalline volcanic ejectum collected at Valle Biachella, Sacrofano community, in the Sabatini volcanic complex, Latium (Italy). We succeeded to obtain a structural model for this mineral, and a formal proposal was submitted the IMA-NMNC Commission, which approved the species and the name (IMA 2009-086). The name kircherite is for Athanasius Kircher (1602 – 1680), a German Jesuit scholar who published around 40 works, some of which dealt with magnetism, geology, mineralogy and volcanology. Athanasius Kircher was in Rome from 1635 and was the founder of the museum of the *Collegium Romanum* in 1651, hereafter named the *Museum Kircherianum*. It contained collections of Roman, Etruscan, and Egyptian antiquities including mummies and large collections of natural objects such as minerals and precious stones. The refined and analyzed crystal is deposited at the Museum of Mineralogy of the "Sapienza" University of Roma (code number MMUR 33035/1). This paper is dedicated to the memory of Luigi Mattei.

OCCURRENCE, PHYSICAL AND OPTICAL PROPERTIES

The holocrystalline volcanic ejectum containing kircherite was collected at Valle Biachella, Sacrofano community. Valle Biachella is a small valley on the inner side of the Sacrofano caldera wall, in the eastern sector of the Sabatini volcanic complex which is

located in northern-central Latium about 20 km to the north of Rome. This complex, together with the other Latian volcanic complexes, belongs to the so-called "Roman Ultrapotassic Province." The Sabatini volcanic complex is characterized by an areal, mainly explosive activity, with the emplacement of numerous eruptive centers, which started about 0.6 Ma ago and ended about 0.08 Ma ago. This activity evolved throughout several caldera collapses and the emission of large volumes of pyroclastic products having the alkaline-potassic signature typical of the Roman Ultrapotassic Province. In Valle Biachella outcrops essentially the "Sacrofano upper pyroclastic flow" unit linked to the volcanic activity of the satellite center of Sacrofano (De Rita et al. 1983, 1993 and references therein).

The ejectum, about 15 cm in size, is a granular but compact rock whitish-gray in color. The groundmass consists of interlocking K-feldspar with minor sodalite, plagioclase, brown mica and andraditic garnet. Fluorite, iron oxides, a pyrochlore-group mineral, and a britholite-like phase are the accessory minerals (Fig. 1a and 1b). Kircherite, which occurs within the interstices between the interlocking K-feldspar, occurs as parallel associations of hexagonal thin tabular shaped crystals (Fig. 2a). The morphology of the kircherite crystals results essentially from the combination of the {00.1} pinacoid with the $\{101;\bar{1}\}$ rhombohedron (Fig. 2b). The maximum size of the crystal groups does not exceed 2 or 3 mm in diameter and up to 1 mm in thickness; the single platelets have a thickness that very rarely exceeds 0.5 mm.

Kircherite appears as transparent to translucent and even opaque in the most altered parts of the material; the luster is greasy to silky and the streak is white. The samples fluoresce light pink under long wave UV and deep red under short wave UV. It is brittle with an uneven fracture and a good cleavage on {00.1}; parting is not observed. The measured density, determined by flotation in a mixture of bromoform-ethanol, is D_{meas} = 2.42 g/cm^3 and the calculated density from the empirical formula is D_{calc} = 2.457 g/cm^3.

Vickers hardness was measured at the Interdepartmental Laboratory of Electron Microscopy (LIME), Università Roma Tre, by means of a Mitutoyo HM-124 microhardness tester, with an applied load of 10 gf (0.1 N) (duration of force 10 s, other test parameters in accordance with ASTM E384 Standard 2008). The average diagonal of the Vickers indent was measured by a Digital Optical Microscope at a magnification of 1000x. Vickers Hardness Number (VHN) was calculated by the following equation: $VHN=1.8544 * (P / d^2)$, where the applied load P is in kgf, the average dimension d of the indentation marks is in mm, with the resulting hardness number expressed in kgf/mm^2. Results showed an average Vickers hardness of 648.4 ± 107 (with a range of 208.9) HV 10 gf (corresponding to about 5.5 in the Mohs scale). It is worth noting that the applied load of 10 gf was selected in order to avoid cracking after indentation, and have a proper evaluation of the actual hardness of the investigated material.

Kircherite is non-pleochroic, negative uniaxial with ω = 1.510(2) and ε = 1.502(2). The refractive indices were determined by the double variation method (see Su et al. 1987 and references therein) and the grain was oriented with the spindle stage so as to measure the refractive indices (Gunter et al. 2005 and references therein).

According to the various studies done in the last decade on the rare minerals which are typically observed in the cavities of the ejecta of Latium (e.g. Della Ventura et al., 1992,1993, 1999, Bellatreccia et al., 2002) the mineral formed during late-stage metasomatic processes related to the volcanic activity.

CHEMICAL COMPOSITION

The composition of kircherite was determined using a JEOL JXA 8200 WD-ED electron microprobe at INGV, Rome. Operating conditions were 15 kV and 4.95 nA, with a beam diameter of 5 μm; counting time was 10 s on both peak and background. Standards, spectral lines, and crystals used were: sodalite (Al*K*α, TAP; Si*K*α, PET; Na*K*α, TAP; Cl*K*α,

PET) augite (Ca*K*α, PET; Mg*K*α, TAP; Fe*K*α, LIF), orthoclase (K*K*α, PET), anhydrite (S*K*α, PET), spessartine (Mn*K*α, LIF), TiO (Ti*K*α, LIF) and fluorite (F*K*α, TAPH). Data reduction used the ZAF correction method. Analytical errors are 1% relative for major elements and 5% relative for minor elements. The crystal fragment used for single-crystal refinement was found to be homogeneous within analytical error. The chemical composition and empirical formula, calculated on the basis of 216 (Si+Al) atoms per formula unit, are given in Table 1; site populations are based on the structure refinement. The simplified ideal charge-balanced formula is: $[Na_{90}Ca_{36}K_{18}]_{\Sigma=144}(Si_{108}Al_{108}O_{432})(SO_4)_{36}\cdot 6H_2O$, which can be expressed as $\{[Na_5Ca_2K]_{\Sigma=8}(Si_6Al_6O_{24})(SO_4)_2\cdot 0.33H_2O\} \times 18$. This requires: K_2O 4.11, Na_2O 13.51, CaO 9.78, Al_2O_3 26.68, SiO_2 31.44, SO_3 13.96, H_2O 0.52, Total 100.00 wt.%. The H_2O content was calculated and checked on the basis of the single-crystal refinement, assuming that the 'cancrinite cages' host only H_2O, and that the $(SO_4)^{2-}$ groups missing to reach 36 per unit cell are substituted by $(CO_3)^{2-}$ + (H_2O) + Cl^- + F^- in the 'losod' and 'sodalite cages' (see structure description); FTIR spectroscopy (see below) showed only H_2O and a small but yet significant amount of CO_2; no OH was detected.

X-RAY DIFFRACTION AND DESCRIPTION OF THE STRUCTURE

The powder X-ray diffraction data of kircherite (Table 2) were collected at the Dipartimento di Scienze Geologiche, Università Roma Tre, with a Scintag X1 diffractometer using: Cu*K*α (λ=1.5418 Å) radiation, fixed divergence slits, and a Peltier-cooled Si(Li) detector (resolution < 200eV). A divergent slit width of 2 mm and a scatter slit width of 4 mm were employed for the beam source; a receiving slit width of 0.5 mm and scatter slit width of 0.2 mm were used for the detector. Data were collected in step-scan mode: 2-60° 2θ range, step-size 0.02° 2θ, counting time 3 s/step. Silicon powder SRM 640d was used as internal standard. The unit–cell parameters, determined using the least

squares refinement program LSUCRIPC (Garvey 1986), are (in Å): a = 12.881(5), c = 95.28(5), V = 13,690(10) Å^3.

Structure determination and refinement

A crystal of 0.73x0.40x0.27 mm was used for single crystal X-ray diffraction on a Bruker AXS Smart Apex diffractometer, with Mo$K\alpha$ (λ = 0.71073 Å) radiation and working at 45 kV and 30 mA, at the Dipartimento di Scienze della Terra e dell'Ambiente, Università di Pavia. The detector-to crystal working distance was 8 cm. Lp and empirical absorption corrections (SADABS, Sheldrick 1998) were applied. The refined unit-cell parameters were obtained from 9259 reflections with $I > 10\sigma(I)$ collected in the 2θ range 5-70º. Ten data sets of 900 images were collected for 5 seconds performing 0.2 ° ω-scans at different ϕ angles (0, 90, 180 and 270° with the detector at θ = 20° and 0, 45, 90, 135, 180 and 270° with the detector at θ = 50°). Indexing of reflections in images was compatible with a rombohedral lattice [a = 12.8767(7), c = 95.244(6) Å, in the hexagonal setting]. Integration in the 2-30° θ-range yielded 81225 reflections compatible with a maximum 3m1 Laue symmetry. The structure was tentatively solved in the space group $R\bar{3}$ by direct methods using SIR 2004 (Burla et al. 2005), which supplied an incomplete model with an R-value of 24.7 %, consisting mainly of framework cations and anions. The structure refinement was completed by adding atoms to the model extracted from Fourier difference maps. This allowed us to find extraframework cations and anionic groups $(SO_4)^{2-}$. We obtained a final model with anisotropic displacement parameters yielding an agreement factor of R = 0.125 for 11517 reflections with $I > 2\sigma(I)$, and R = 0.135 for all 13437 unique reflections. There were 12 four-fold coordinated cations composing the framework; and no Si-Al ordering was found. The observed staking sequence in the hexagonal cell, following the Zhdanov notation (Zhdanov, 1945; Patterson and Kasper, 1959), was:

207 – + + + + + + + + + + + – – + + + + + + + + + + + – – + + + + + + + + + + + –
(A) C A B C A B C A B C A (C) B C A B C A B C A B C (B) A B C A B C A B C A B (A)
0 1 2 3 4 5 6 7 8 9 10 11 12 13 14 15 16 17 18 19 20 21 21 23 24 25 26 27 28 29 30 31 32 33 34 35 36

208

209 …, where A, B and C represent the position of rings of tetrahedra within layers. The

210 sequence for the rhombohedral cell is given below.

211 – + + + + + + + + + + + –
(A) C A B C A B C A B C A [C]
0 1 2 3 4 5 6 7 8 9 10 11 12

212

213 Therefore the sequence is expressed as an even period (12) and a different basic partition

214 (i.e., 3 × 12 [(10)(2)]), and thus, following Patterson and Kasper (1959), should have a

215 rhombohedral lattice. Both successions are centrosymmetric and both centers are in

216 spheres. Therefore the space group should be $R\bar{3}m$. However, so far all the cancrinite

217 related minerals (but cancrsilite, where the Si:Al is not 1:1) have shown Si-Al ordering

218 among the tetrahedral sites, and the $R\bar{3}m$ space group would not allow for such ordering.

219 Therefore we tried to lower the symmetry to that of space group $R3$. This model converged

220 to a lower *R*-index (0.108). It had 24 four-fold sites this time showing ordering of Al and Si

221 in 12 sites, respectively. Testing this model with PLATON/addsym (Spek 2008) yielded a

222 higher symmetry model in $R32$ with 14 fourfold sites in the framework (7 Al + 7 Si sites).

223 Refining for the presence of inversion center yielded 0.57(9) of merohedral twining.

224 Refinement of this model produced better <Al-O> and <Si-O> distances and maintained

225 the Al and Si ordered. Although we cannot rule out a center of symmetry, the model with

226 symmetry $R\bar{3}$ showed no ordering; thus, we kept the highest symmetry allowing ordering of

227 Al and Si. Refinement converged to $R = 0.084$ for 8131 reflections with $I > 2\sigma(I)$, and $R =$

228 0.088 for all 8908 unique reflections [$R_{int} = 0.0308$, 69 restraints and 515 parameters,

229 Goodness of fit on $F^2 = 1.056$]. The framework of tetrahedra builds up a series of cages,

230 which are filled by cations and anions/anionic groups. The observed cage topologies are

231 'cancrinite cages' (ε), [$4^3 6^5$] in the IUPAC nomenclature (McCusker et al. 2001), [$4^6 6^8$]

'sodalite cages', and [$4^6 6^{11}$] 'losod cages'. The extraframework cation positions showed strong static disorder and therefore we chose to refine those as split sites. Displacement parameters of atoms in a split site were constrained to be equal. The model also has 6 anionic groups: 2 out of them (those located at the 'losod cages', see description of the structure) are ordered; four are located in 'sodalite cages' in off-axis positions and were refined with isotropic displacement parameters. Careful search for maxima in the Fourier-difference maps allowed location of some of the oxygen atoms at the vertexes of the $(SO_4)^{2-}$ groups. These were added to the model and refined with a soft constraint on the bond-length; in order to let the model to reach a minimum, displacement parameters were constrained to be equal to those observed for the ordered $(SO_4)^{2-}$ groups. Final atomic coordinates and equivalent isotropic displacement parameters are given in Table 4, selected distances for framework cations in Table 5a and selected distances for extra-framework cations and anionic groups in Table 5b and 5c (the CIF has been deposited as electronic supplemental material).

FTIR Spectroscopy

The powder FTIR spectrum of kircherite was collected at the Dipartimento di Scienze Geologiche, Università Roma Tre on a Nicolet Magna 760 FTIR spectrometer equipped with a DTGS detector and a KBr beamsplitter; the nominal resolution was 4 cm^{-1} and 64 scans were averaged for each sample and for the background. The spectrum was collected on a KBr disk with about 1 mg of sample in 150 mg of KBr. Single-crystal FTIR spectra were collected on crystal fragments ~ 30 μm thick using a NicPlan microscope equipped with a liquid nitrogen-cooled MCT detector; the nominal resolution was 4 cm^{-1} and 128 scans were averaged for each sample and for the background.

The infrared powder spectrum of kircherite (Fig. 3a) shows a broad absorption from 3740 cm^{-1} to 3000 cm^{-1} due to the stretching modes plus the bending overtone (ν_1, ν_3 and

258 $2\nu_2$) of the H_2O molecule(s) and at 2338 cm^{-1} a small but sharp absorption assigned to the
259 stretching mode (ν_3) of the CO_2 molecules (Della Ventura et al. 2005, 2007, 2008). This
260 value is in the range observed for CO_2 bearing cancrinite group minerals, where the
261 wavenumber of this band has been observed to vary from 2338 cm^{-1} for fantappièite
262 (Cámara et al. 2010) up to 2352 cm^{-1} for marinellite (Bellatreccia et al. 2007). In the
263 frequency region from 400 to 1750 cm^{-1} (Fig. 3b) there is a broad band due to the bending
264 mode (ν_2) of the H_2O molecule at 1635 cm^{-1} and a multi-component strong band at 1200-
265 1000 cm^{-1}, which can be assigned to the stretching modes of the $(SO_4)^{2-}$ and TO_4 groups
266 (Moenke 1974; Ross 1974). A sharp but very weak absorption is observed at 1384 cm^{-1}
267 which can be assigned to $(CO_3)^{2-}$ groups. A group of well-defined bands occur in the range
268 800-500 cm^{-1}; in particular, six absorptions at 698, 651, 609, 590, 546 and a shoulder at
269 737 cm^{-1} are resolved. Finally, a very intense and convoluted absorption is observed at
270 around 446 cm^{-1}. As already discussed in previous papers (e.g., Ballirano et al. 1996a;
271 Cámara et al. 2005, 2010) this spectral region is characteristic of any cancrinite group
272 species and is useful for identification purposes. In this particular case, although being
273 typical of kircherite, it shows some similarities with the spectra of haüyne, franzinite and
274 fantappiéite (Ballirano et al. 1996a; Cámara et al. 2005, 2010).
275 The single-crystal FTIR spectrum was collected in the 6000-650 cm^{-1} range; the
276 4000 to 1500 cm^{-1} region is displayed in Figure 5. It shows a very intense multi-component
277 band which can be resolved into three main components at 3527 cm^{-1}, 3412 cm^{-1} and
278 3246 cm^{-1} which can be assigned to the stretching modes (ν_1 and ν_3) and the first bending
279 overtone ($2\nu_2$) of the H_2O molecule(s), respectively. The spectrum also shows a very
280 sharp absorption at 2338 cm^{-1} which confirm the presence of CO_2 molecules in the
281 structural pores of kircherite (Della Ventura et al. 2005, 2007, 2008). The broad absorption
282 at 2125 cm^{-1} can be assigned to the first overtone or combination modes of the T-O bonds
283 and to the first overtone of the asymmetric stretching mode (ν_3) of the $(SO_4)^{2-}$ group (Della

Ventura et al. 2008). The strong absorption at 1636 cm^{-1} is due to the H_2O bending mode (ν_2) and the shoulder at 1687 cm^{-1} can be attributed to combination of T-O modes. Finally, a broad absorption at around 5234 cm^{-1} (not shown) is assigned to the combination of the stretching (ν_3) + bending (ν_3) modes of H_2O (Ihinger et al. 1994). The absence of bands in the 4300-4100 cm^{-1} range (inset in Fig. 5), due to the combination modes of the in OH group (Ihinger et al. 1994), rules out the presence of hydroxyl groups in kircherite.

DESCRIPTION OF THE CRYSTAL STRUCTURE

The structure has six 'cancrinite cages' (ε), [$4^3 6^5$] in the IUPAC nomenclature (McCusker et al. 2001), 24 [$4^6 6^8$] 'sodalite cages' (S), and 6 [$4^6 6^{11}$] 'losod cages' (Lo) within the unit cell. There is a unique sequence of cages, and adjacent sequences are shifted 1/3 along [00.1]. Different types of cages are ordered as εSSSLoSSLoSSSε (Fig. 6).

Cancrinite (ε) cages

Cancrinite cages contain (H_2O) groups, which coordinate Na atoms at Na1 site in the 6mR ⊥ [00.1] window shared by two consecutive ε-cages and to Ca atoms at the other 6mR ⊥ [00.1] windows with long and weak bonds (2.93 Å). Refined site scattering is compatible with almost full occupancy of H_2O in one on-axis position completing the ditrigonal pyramid corresponding to the Na coordinating environment. There are 6 ε cages per unit cell, which accounts for 6 H_2O p.f.u.

Losod cages

Six [$4^6 6^{11}$] cages (losod cages) are present p.f.u., which match with two sodalite cages ([$4^6 6^8$]) along [00.1]. The losod cage occurs in many members of the group: bystrite and carbobystrite, liottite (Ballirano et al. 1996b), franzinite, tounkite, biachellaite, fantappiéite, sacrofanite, and obviously kircherite. In kircherite, each losod cage contains

two $(SO_4)^{2-}$ groups ordered with apexes pointing oppositely along [00.1], which coordinate 3 K atoms off-axis in the plane between the bases of the two $(SO_4)^{2-}$ groups, Ca atoms at the Ca3 site in one of the 6mR ⊥ [00.1] windows and Ca and minor Na atoms at the Ca7 site centered approximately at the other the 6mR ⊥ [00.1] window. Na and Ca at the Na2 and Na4 sites in the center of the six membered rings in the wall of the cage (hereafter 6mR || [00.1]) also coordinates with the oxygen apexes of the $[(S1)O_4]^{2-}$ and $[(S2)O_4]^{2-}$ anionic groups, respectively. These two cation positions have different occupancy as a function of the anion located at the center of the adjacent sodalite cages.

Sodalite cages

Sodalite cages ($[4^6 6^8]$) are the most frequent cages in kircherite (up to 24 sodalite cages per unit cell). They mostly contain $(SO_4)^{2-}$ groups disordered so that it was not possible to find the position of all oxygen atoms in the four symmetrically independent sites. This disorder is common in all the minerals of the cancrinite group showing this type of cage, usually containing sulfate groups in more than one orientation, as well as split cation sites in the two 6mR ⊥ [00.1] and the six 6mR || [00.1] windows that may host Na or Ca cations. Sodalite cages also contain minor Cl (and F) that coordinates Ca and (H_2O) which coordinates Na (up to complete 36 anion groups and anions per formula unit; see Table 6). Therefore the composition of sodalite cages are mostly related to haüynic and to a lesser degree sodalitic and noseanic. The white color of kircherite probably excludes the presence of $(S_3)^-$ at the sodalitic cages, which usually results in the blue coloration of these minerals (Ostroumov et al. 2002; Fleet et al. 2005). Overall, the number and type of cages in the unit cell account for a maximum of 36 $(SO_4)^{2-}$ groups and 6 (H_2O) molecules (or Cl^- anions).

Site assignment

Assigned site population on the basis of observed site scattering and site geometry (i.e., bonding environment) is reported Table 6. There is a slight disagreement between

the Ca + K assignments based on the refinement as compared to that determined by electron microprobe. However, considering the similar scattering power of both atomic species, the observed disagreement might be ascribed to erroneous assignment of elements to these sites, which is done on the basis of the mean bond lengths, as the bonding environments put some restrictions to the occupying species on the basis of their ionic radii. Considering the large cell, the complexity of the structure and the observed *R*-factor, the disagreement should be ascribed to difficulties on refining the split positions thus leading to local geometries incompatible for Ca population or excess observed site scattering. Disagreement with the calculated site scattering for cation sites from EMP analyses is 7.8%. This is the case in particular for the split sites K6B, K9B, K1G and K1L, which account for 17.53 K apfu; their bonding environment is too large for Ca and Na.

Considering the extraframework composition obtained by EMP analyses and the dominant anionic species or groups in the cages, the simplified ideal charge-balanced formula is: $[Na_{90}Ca_{36}K_{18}]_{\Sigma=144}(Si_{108}Al_{108}O_{432})(SO_4)_{36}\cdot 6H_2O$, which can be expressed as $\{[Na_5Ca_2K]_{\Sigma=8}(Si_6Al_6O_{24})(SO_4)_2\cdot 0.33H_2O\}*18$. This requires: K_2O 4.11, Na_2O 13.51, CaO 9.78, Al_2O_3 26.68, SiO_2 31.44, SO_3 13.96, H_2O 0.52, Total 100.00 wt.%.

The compatibility indices (Mandarino 1981) are: $(1 - K_P)/K_C$ = -0.022 (i.e., excellent) by using $D_{calc,}$ and $(1 - K_P)/K_C$ = -0.038 (i.e., excellent) by using D_{meas}, indicating excellent agreement between physical and chemical data.

RELATION TO OTHER SPECIES

Kircherite is a new mineral of the cancrinite-sodalite group and is a member of the subgroup with a complex sequence. Within this subgroup, kircherite, having 36 layers (in the hexagonal setting; 12 in the rhombohedral), is the cancrinite with the longest complex sequence described to date. Considering the rhombohedral setting, it is the third mineral of the cancrinite-sodalite group showing 12 layers sequence, along with tounkite (Rozenberg

et al. 2004) and marinelite (Bonaccorsi and Orlandi 2003). The three structures have very different layers sequences, Zhdanov symbol and number and type of cages:

Marinelite:	ABCBCBACBCBC	|1(4)1|1(4)1|	2 lio, 4 sod, 6 ε
Tounkite:	ABABACACABAC	(2)211(2)211	2 lio, 2 sod, 8 ε
Kircherite:	ACABCABCABCA	[(10)(2)]	2 los, 8 sod, 2 ε

being lio = 'liottite cages' [$4^6 6^{17}$]. The different topology in terms of cages constrain the chemistry of the three different minerals. Nevertheless, a correct identification cannot be done on the basis of only a chemical analysis, and requires a X-ray diffraction.

Careful inspection of the sequence (Fig. 6) reveals that the structure of kircherite can be derived from that of sodalite by inserting a shifted layer every 11 layers, as for fantappièite and franzinite. In the case of fantappièite the structure can be obtained from sodalite by inserting a shifted layer every 10 layers [sequence (9)(2)], and from franzinite by inserting a shifted layer every 9 layers [sequence (8)(2)]. Therefore, kircherite represents the third member of a particular subgroup in which ordered interstratified sodalite-cancrinite sequences are found to follow the scheme: (*n*sod)(can), for *n* = 1, 2, 3, 4, … Expected sequences are (3)(2), (4)(2), (5)(2), (6)(2), (7)(2), (8)(2), (9)(2), (10)(2),…, of which the last three have been discovered. Two of these have hexagonal cells [i.e., (5)(2) and (8)(2)], while the remainder have rhombohedral cells and therefore sequences of 15, 18, 24, 27, 33 and 36 layers in the hexagonal setting, corresponding to *c* axis lengths of *ca* 39.7, 47.6, 63.5, 71.4, 87.3, and 95.2 Å.

ACKNOWLEDGEMENTS

Thanks are due to late Mr. Luigi Mattei who provided us with the sample allowing the discovery of this new mineral. Roberto Gastoni CNR-IGG of Pavia (Italy) assisted with sample preparation for EMPA. FC thanks the Dipartimento di Scienze della Terra e dell'Ambiente, Università di Pavia (Italy) and CNR-IGG of Pavia (Italy) for granting access

to the single-crystal diffractometer. The suggestions of two anonymous reviewers and Associate Editor Fernando Colombo helped to improve the quality of the manuscript.

REFERENCES

ASTM Standard E384 08ae1 (2008) Standard Test Method for Microindentation Hardness of Materials. ASTM International, West Conshohocken, PA, DOI: 10.1520/E0384-08AE01, www.astm.org.

Ballirano, P., Maras, A., and Buseck, P.R. (1996a) Crystal chemistry and IR spectroscopy of Cl^- and SO_4^{2-} bearing cancrinite-like minerals. American Mineralogist, 81, 1003-1012.

Ballirano, P., Merlino, S., Bonaccorsi, E., and Maras, A. (1996b) The crystal structure of liottite, a six-layer member of the cancrinite group. Canadian Mineralogist, 34, 1021-1030.

Ballirano, P., Bonaccorsi, E., Maras, A., and Buseck, P.R. (1997) The crystal structure of afghanite, the eight-layer member of the cancrinite group: evidence for long-range Si, Al ordering. European Journal of Mineralogy, 9, 21-30.

Bellatreccia, F., Della Ventura, G., Williams, T.C., Lumpkin, G.R., Smith, K.L., and Colella, M. (2002) Non-metamict zirconolite polytypes from the feldspathoid-bearing alkali-syenitic ejecta of theVico volcanic complex (Latium, Italy). European Journal of Mineralogy, 14, 809-820.

Bellatreccia, F., Della Ventura, G., Parodi, G.C., Pucci, R., and Mattei, L. (2007) New data on marinellite, a mineral of the cancrinite-sodalite group. Geoitalia 2007. Sesto Forum Italiano di Scienze della Terra. Rimini, 12-14 settembre 2007, Epitome, 1050.

Bonaccorsi, E. and Merlino, S. (2005) Modular microporous minerals: cancrinite-davyne group and CSH phases. In G. Ferraris and S. Merlino (Eds.), Micro and mesoporous mineral phases, p. 241-290. Reviews in Mineralogy and Geochemistry, Mineralogical Society of America and the Geochemical Society, Washington, D.C.

Bonaccorsi, E. and Orlandi, P. (2003) Marinellite, a new felspatoid of the cancrinite-sodalite group. European Journal of Mineralogy, 15, 1019-1027.

Bonaccorsi, E., Ballirano, P., and Cámara F. (2012) The crystal structure of sacrofanite, the 74 Å phase of the cancrinite-sodalite supergroup. Microporous & Mesoporous Materials, 147, 318-326.

Burla, M.C., Caliandro, R., Camalli, M., Carrozzini, B., Cascarano, G.L., De Caro, L., Giacovazzo, C., Polidoria, G., and Spagna, R. (2005) SIR2004: an improved tool for crystal structure determination and refinement. Journal of Applied Crystallography, 38, 381-388.

Cámara, F., Bellatreccia, F., Della Ventura, G., and Mottana, A. (2005) Farneseite, a new mineral of the cancrinite - sodalite group with a 14-layer stacking sequence: occurrence and crystal structure. European Journal of Mineralogy, 17, 839-846.

Cámara, F., Bellatreccia, F., Della Ventura, G., Mottana, A., Bindi, L., Gunter, M.E., and Sebastiani, M. (2010) Fantappièite, a new mineral of the cancrinite - sodalite group with a 33-layer stacking sequence: occurrence and crystal structure. American Mineralogist, 95, 472-480.

Chukanov, N.V., Rastsvetaeva, R.K., Pekov, I.V., and Zadov, A.E. (2007) Alloriite, $Na_5K_{1.5}Ca(Si_6Al_6O_{24})(SO_4)(OH)_{0.5}$ H_2O,a new mineral species of the cancrinite group. Geology of Ore Deposits, 49, 752–757.

Chukanov, N.V., Rastsvetaeva, R.K., Pekov, I.V., Zadov, A.E., Allori, R., Zubkova, N.V., Giester, G., Pushcharovsky, Yu, D., and Van, K.V. (2008) Biachellaite $(Na,Ca,K)_8(Si_6Al_6O_{24})(SO_4)_2(OH)_{0.5}.H_2O$, a new mineral of the cancrinite group. Proceedings of the Russian Mineralogical Society, 137(3),57–66 (Russian with English abstract).

439 Della Ventura, G., Di Lisa, A., Marcelli, M., Mottana, A., and Paris, E. (1992) Composition
440 and structural state of alkali feldspars from ejecta in the Roman potassic province,
441 Italy; petrological implications. European Journal of Mineralogy, 4, 411-424.
442 Della Ventura, G., Parodi, G.C., Mottana A., and Chaussidon, M. (1993) Peprossiite (Ce),
443 a new mineral from Campagnano (Italy): the first anhydrous rare-earth-element
444 borate. European Journal of Mineralogy, 5, 53-58.
445 Della Ventura, G., Williams, T.C., Cabella, R., Oberti, R., Caprilli, E., and Bellatreccia, F.
446 (1999) Britholite - hellandite intergrowths and associated REE-minerals from the
447 alkali-syenitic ejecta of the Vico volcanic complex (Latium, Italy): petrological
448 implications bearing on REE mobility in volcanic systems. European Journal of
449 Mineralogy, 11, 843-854.
450 Della Ventura, G., Bellatreccia, F., and Bonaccorsi, E. (2005) CO_2 in minerals of the
451 cancrinite-sodalite group: pitiglianoite. European Journal of Mineralogy, 17, 847-
452 851.
453 Della Ventura, G., Bellatreccia, F., Parodi, G.C., Cámara, F., and Piccinini, M. (2007)
454 Single-crystal FTIR and X-ray study of vishnevite, ideally
455 $[Na_6(SO_4)][Na_2(H_2O)_2](Si_6Al_6O_{24})$. American Mineralogist, 92, 713-721.
456 Della Ventura, G., Bellatreccia, F., and Piccinini, M. (2008) Channel CO_2 in feldspathoids:
457 new data and new perspectives. Rendiconti Lincei 19, 141-159.
458 De Rita D., Funiciello R., Rossi U., and Sposato A. (1983) Structure and evolution of the
459 Sacrofano-Baccano caldera, Sabatini volcanic complex, Rome. Journal of
460 Volcanology and Geothermal Research, 17, 219-236.
461 De Rita D., Funiciello R., Corda L., Sposato A., and Rossi U. (1993) Volcanic Units. In:
462 Sabatini Volcanic Complex (Ed. M. Di Filippo). Quaderni de “La ricerca scientifica’’,
463 114, Progetto Finalizzato "Geodinamica", monografie finali, 11: 33-79.

Fleet, M. E., Liu, X., Harmer, S. L., and Nesbitt, H.W. (2005) Chemical state of sulfur in natural and synthetic lazurite by S K-edge Xanes and X-ray photoelectron spectroscopy. Canadian Mineralogist, 43, 1589-1603.

Garvey R.G. (1986) LSUCRIPC, least squares unit-cell refinement with indexing on the personal computer. Powder Diffraction 1, 89.

Gunter, M.E., Downs, R.T., Bartelmehs, K.L., Evans, S.H., Pommier, C.J.S., Grow, J.S., Sanchez, M.S., and Bloss, F.D. (2005) Optic properties of centimeter-sized crystals determined in air with the spindle stage using EXCALIBRW. American Mineralogist, 90, 1648-1654.

Ihinger, P.D., Hervig, R.L., and McMillan. P.F. (1994) Analytical methods for volatiles in glasses. In M.R. Carroll and J.R. Holloway, Eds., Volatiles in Magmas, p. 67-121. Reviews in Mineralogy, Mineralogical Society of America, Washington, D.C.

Khomyakov, A.P., Cámara, F., and Sokolova, E. (2010) Carbobystrite, $Na_8[Al_6Si_6O_{24}](CO_3)•4H_2O$, a new cancrinite-group mineral species from the Khibina alkaline massif, Kola peninsula, Russia: description and crystal structure. Canadian Mineralogist, 48, 291-300.

Mandarino, J.A. (1981) The Gladstone-Dale relationship: Part IV. The compatibility concept and its application. Canadian Mineralogist, 19, 441-450

McCusker, L.B., Liebau, F., and Engelhardt, G. (2001) Nomenclature of structural and compositional characteristics of ordered microporous and mesoporous materials with inorganic hosts. Pure Applied Chemistry, 73, 381-394.

Moenke, H.H.W. (1974) Silica, the three-dimensional silicates, borosilicates and beryllium silicates. In V.C. Farmer (Ed.), The infrared spectra of Minerals, 365-382. The Mineralogical Society, London.

Ostroumov, M., Fritsch, E., Faulques, E., and Chauver, O. (2002) Etude spectrometrique de la lazurite du Pamir, Tajikistan. Canadian Mineralogist, 40, 885-893.

Patterson, A.L. and Kasper, J.S. (1959) Close packing. *In* International Tables for X-ray Crystallography, Vol II, The Kynoch Press, Birmingham, 342-354.

Rastsvetaeva, R.K. and Chukanov, N.V. (2008) Model of the crystal structure of biachellaite as a new 30-layer member of the cancrinite group. Crystallography Reports, 53, 981-988.

Rastsvetaeva, R.K., Ivanova, A.G., Chukanov, N.V., and Verin, I.A. (2007): Crystal structure of alloriite. Doklady Earth Sciences, 415, 815–819.

Rinaldi, R. and Wenk, H.R. (1979) Stacking variations in cancrinite minerals. Acta Crystallographica, A35, 825-828.

Ross, S.D. (1974) Sulphates and other oxy-anions of Group VI. In V.C. Farmer (Ed.), The infrared spectra of Minerals, 423-444. The Mineralogical Society, London.

Rozenberg, K.A, Sapozhnikov, A.N., Rastsvetaeva, R.K., Bolotina, N.B., and Kashaev, A.A. (2004) Crystal structure of a new representative of the cancrinite group with a 12-layer stacking sequence of tetrahedral rings. Crystallography Reports, 49, 635-642.

Sheldrick, G.M. (1998) SADABS. Bruker AXS Inc., Madison, Wisconsin, USA.

Spek, A.L. (2008) PLATON, A Multipurpose Crystallographic Tool, Utrecht University, Utrecht, The Netherlands.

Su, S.C., Bloss, F.D., and Gunter, M.E. (1987) Procedures and computer programs to refine the double variation method. American Mineralogist, 72, 1011-1013.

Zhdanov, G.S. (1945) The numerical symbol of close packing of spheres and its application in the theory of close packings. Comptes rendus de l'Académie des Sciences de l'Union des Républiques Soviétiques Socialistes, 48, 39-42.

TABLE CAPTIONS

Table 1. Chemical composition determined using electron microprobe (mean of 18 analyses) and empirical formula of kircherite calculated on the basis of Σ(Si+Al) = 216 apfu.

Table 2. Powder X-ray diffraction data for kircherite.

Table 3. Crystal data and structure refinement for kircherite.

Table 4. Atomic coordinates and equivalent isotropic displacement parameters ($Å^2$) for framework cations and anions in kircherite.

Table 4 ctd. Atomic coordinates and equivalent isotropic displacement parameters ($Å^2$) for extraframework cations and anions in kircherite.

Table 5a. Selected distances of framework cations for kircherite.

Table 5b. Selected distances of extra-framework cations sites for kircherite.

Table 5c. Selected distances of extra-framework anionic groups for kircherite.

Table 6. Cation site assignments on the basis of observed site scattering and geometries of the sites reported in Table 5 for kircherite

FIGURE CAPTIONS

Fig. 1. Photomicrographs (crossed polars) of kircherite in thin section: a) kircherite (kir) with k-feldspar (Kf) and biotite (bio); b) typically twinned crystals of kircherite.

Fig. 2. a) Photomicrographs and b) morphological sketch of kircherite (sample and photo L. Mattei).

Fig. 3. FTIR powder spectrum of kircherite: a) H_2O (stretching) and CO_2 absorptions (* = grease); b) low frequency region with the H_2O (bending), SO_4^{2-}, trace of CO_3^{2-} and the typical $(Si,Al)O_4$ absorptions (see text for explanations).

Fig. 4. The FTIR powder spectrum of kircherite compared to the spectra of haüyne, franzinite, and fantappièite.

Fig. 5. The single-crystal unpolarized-light FTIR spectrum of kircherite; NIR region in the inset.

Fig. 6. Projection of the kircherite structure along [112;$\bar{}$0] showing the stacking sequence of cages along [00.1] at (0,0,z). ε: 'cancrinite cage' (gray); s: 'sodalite cage' (light gray); los: 'losod cage' (dark gray). Si: dark gray spheres; Al: light gray spheres.

Table 1. Chemical composition determined using electron microprobe (mean of 18 analyses) and empirical formula of kircherite calculated on the basis of Σ(Si+Al) = 216 apfu.

	Wt.%	Range		apfu
SiO_2	32.05	31.17-33.31	Si	108.13
Al_2O_3	27.13	26.66-27.62	Al	107.87
FeO	0.07	0.00-0.18	Σ	216.00
K_2O	4.38	4.15-4.62		
CaO	8.75	8.48-9.29	Ca	31.63
Na_2O	13.62	12.66-14.02	Fe^{2+}	0.20
MgO	0.01	0.00-0.05	K	18.85
MnO	0.02	0.00-0.08	Na	89.09
TiO_2	0.01	0.00-0.05	Ti	0.03
SO_3	12.87	12.61-13.46	Mg	0.05
Cl	0.35	0.28-0.42	Mn	0.06
F	0.05	0.00-0.20	Σ	139.91
$H_2O^{‡}$	0.61	0.74-0.44		
	99.92	98.75-102.02	SO_4^{2-}	32.58
O=F,Cl	0.10	0.06-0.16	Cl^-	2.00
Total	99.82	98.65-101.86	F^-	0.53
			$H_2O^{‡}$	6.86
			O	430.19

‡ Calculated on the basis of the single-crystal refinement (see text).

Table 2. Powder X-ray diffraction data for kircherite.

I/I_0 (%)	d_{meas} (Å)	d_{calc} (Å)	*hkl*	I/I_0 (%)	d_{meas} (Å)	d_{calc} (Å)	*hkl*
4	31.75	31.76	003	12	2.914	2.914	3,1,11
3	15.88	15.88	006	7	2.886	2.887	0,0,33
10	11.10	11.08	101	2	2.843	2.849	1,1,30; 1,3,13
5	10.85	10.86	012	5	2.817	2.817	3,1,14
15	10.04	10.10	104	4	2.783	2.784	042; 401
2	9.461	9.627	015	4	2.766	2.766	1,2,26; 045
3	6.868	6.842	0,1,11	3	2.751	2.751	2,2,18; 1, 3, 16
17	6.440	6.440	110	100	2.648	2.648	2,1,28; 0,0,36
11	5.809	5.810	0,1,14	3	2.603	2.606	4,0,13
4	5.576	5.568	021	7	2.577	2.581	0,4,14
2	5.460	5.431	024	3	2.549	2.545	324; 235
3	5.292	5.293	0,0,18	3	2.516	2.515	327; 1,0,37
3	5.248	5.253	1,0,16	2	2.499	2.501	2,2,24; 0,4,17
2	5.075	5.051	208	3	2.466	2.472	3,2,10
3	5.012	5.008	0,1,17	5	2.451	2.448	1,1,36; 2,0,35
6	4.792	4.814	0,2,10	5	2.434	2.434	410; 1,2,32
3	4.697	4.689	2,0,11	3	2.408	2.407	0,4,20; 416
3	4.572	4.574	1,0,19	3	2.401	2.402	1,3,25; 2,3,14
3	4.421	4.439	0,2,13	2	2.352	2.351	3,2,16
3	4.329	4.314	2,0,14	6	2.250	2.251	4,0,25; 3,1,29
7	4.215	4.212	211; 122	7	2.168	2.172	0,5,10; 1,0,43
3	4.157	4.152	214	17	2.156	2.157	4,0,28
7	4.107	4.117	125	21	2.147	2.145	3,1,32
7	4.090	4.089	1,1,18	12	2.141	2.140	1,1,42; 333
4	4.070	4.071	0,2,16	3	2.045	2.045	2,2,36; 3,1,35
6	4.037	4.037	1,0,22	3	2.040	2.042	3,0,39; 0,5,19
3	3.983	3.975	128	3	2.003	2.003	511; 152; 4,1,27
3	3.945	3.954	2,0,17	2	1.954	1.952	1,5,11; 0,4,35
52	3.799	3.791	1,2,11	4	1.926	1.926	1,2,44; 4,2,20; 0,5,25
100	3.717	3.718	300	18	1.916	1.916	1,0,49
3	3.657	3.655	2,1,13	3	1.878	1.878	0,1,50
53	3.604	3.607	1,0,25	3	1.873	1.868	0,0,51
60	3.584	3.584	1,2,14	3	1.865	1.866	0,5,28; 2,3,35
24	3.551	3.529	0,0,27	3	1.834	1.834	431; 3,3,27
5	3.466	3.482	0,1,26	3	1.830	1.831	609; 434
5	3.445	3.441	2,1,16	3	1.825	1.825	345; 5,1,22
8	3.370	3.369	1,2,17	2	1.818	1.817	437; 3,2,37
9	3.353	3.367	3,0,12	6	1.796	1.794	1,1,51; 3,4,11
19	3.313	3.326	2,0,23	7	1.793	1.792	2,4,28; 4,1,36
13	3.252	3.255	1,0,28	5	1.787	1.786	520; 5,0,32
65	3.232	3.227	2,1,19	3	1.646	1.646	1,3,49; 6,0,27
38	3.220	3.220	220	11	1.633	1.631	2,4,37; 5,1,34
11	3.152	3.152	0,1,29; 0,2,25	3	1.614	1.614	4,3,28; 1,5,35
9	3.050	3.043	3,0,18	8	1.610	1.610	440; 3,2,46
8	3.021	3.021	2,1,22	4	1.606	1.605	6,0,30; 2,1,55
6	2.994	2.995	318	2	1.573	1.572	0,5,43; 7,0,10
5	2.944	2.943	1,3,10	3	1.568	1.567	0,7,11; 1,5,38

Table 3. Crystal data and structure refinement for kircherite.

Temperature	293(2) K	
Wavelength	0.71073 Å	
Crystal system	Trigonal	
Space group	*R*32	
Unit cell dimensions	a = 12.8770(7) Å	α = 90°
	b = 12.8770(7) Å	β = 90°
	c = 95.244(6) Å	γ = 120°
Volume	13677.2(13) Å^3	
Z	1	
Density (calculated)	2.383 Mg/m^3	
Crystal size	0.73 x 0.40 x 0.27 mm^3	
Theta range for data collection	1.28 to 30.03°.	
Index ranges	-18<=h<=17, -18<=k<=18, -133<=l<=133	
Reflections collected	81125	
Independent reflections	8900 [$R_{(int)}$ = 0.0308]	
Completeness to theta = 30.03°	99.7 %	
Refinement method	Full-matrix least-squares on F^2	
Data / restraints / parameters	8900 / 10 / 510	
Goodness-of-fit on F^2	1.038	
Final *R* indices [I>2sigma(I)]	$R1$ = 0.0847, wR^2 = 0.2304	
R indices (all data)	$R1$ = 0.0893, wR^2 = 0.2370	
Absolute structure parameter	0.53(9)	
Largest diff. peak and hole	3.246 and -2.136 e.Å^{-3}	

Table 4. Atomic coordinates and equivalent isotropic displacement parameters ($Å^2$) for framework cations and anions in kircherite.

Atom	Wyck.	*x/a*	*y/b*	*z/c*	U(eq)
Si1	9d	0.25209(13)	0	0	0.0153(4)
Si2	18f	0.92141(11)	0.58468(10)	0.028745(16)	0.0138(3)
Si3	18f	0.25017(11)	-0.00038(10)	0.056598(17)	0.0153(3)
Si4	18f	0.33285(11)	0.41471(13)	0.084480(16)	0.0165(3)
Si5	18f	0.41674(13)	0.08479(13)	0.112132(17)	0.0176(3)
Si6	18f	0.24895(14)	0.24891(14)	0.139370(16)	0.0180(3)
Si7	9e	1/3	0.91414(17)	1/6	0.0189(4)
Al1	9d	0	0.74422(14)	0	0.0150(4)
Al2	18f	0.40708(12)	0.08485(12)	0.028747(18)	0.0155(3)
Al3	18f	0.25229(13)	0.25532(13)	0.056187(18)	0.0151(3)
Al4	18f	0.33367(13)	0.91923(15)	0.084777(19)	0.0184(4)
Al5	18f	0.41672(15)	0.33299(12)	0.111910(18)	0.0179(4)
Al6	18f	0.24778(16)	-0.00033(13)	0.139511(19)	0.0206(4)
Al7	9e	0.58118(19)	0.91451(19)	1/6	0.0189(5)
O1	18f	0.1218(4)	0.8853(4)	0.00247(3)	0.0257(6)
O2	18f	0.3374(3)	0.0159(4)	0.01327(4)	0.0216(8)
O3	18f	0.9782(4)	0.6459(4)	0.01398(4)	0.0265(10)
O4	18f	0.7830(3)	0.5489(3)	0.03041(3)	0.0241(6)
O5	18f	0.5400(4)	0.0786(3)	0.02974(3)	0.0273(6)
O6	18f	0.0006(4)	0.6698(5)	0.04121(5)	0.0293(10)
O7	18f	0.3192(4)	-0.0016(4)	0.04249(5)	0.0270(9)
O8	18f	0.1132(4)	0.8975(4)	0.05576(3)	0.0284(6)
O9	18f	0.2539(3)	0.1258(4)	0.05938(3)	0.0286(6)
O10	18f	0.3256(5)	0.9846(4)	0.06921(5)	0.0336(11)
O11	18f	0.3276(5)	0.3547(5)	0.06976(6)	0.0379(11)
O12	18f	0.4495(4)	0.8905(3)	0.08400(4)	0.0354(7)
O13	18f	0.2192(4)	0.4260(4)	0.08817(4)	0.0368(8)
O14	18f	0.3496(6)	0.3371(5)	0.09634(6)	0.0413(12)
O15	18f	0.3505(6)	0.0155(7)	0.09803(7)	0.0561(18)
O16	18f	0.4517(5)	0.2220(5)	0.11056(5)	0.0530(11)
O17	18f	0.5372(6)	0.0802(5)	0.11528(5)	0.0554(12)
O18	18f	0.3335(8)	0.0189(7)	0.12516(8)	0.077(3)
O19	18f	0.3153(7)	0.3075(7)	0.12514(7)	0.0612(19)
O20	18f	0.1171(5)	0.2216(6)	0.13723(5)	0.0691(17)
O21	18f	0.2402(6)	0.1267(6)	0.14278(6)	0.0774(19)
O22	18f	0.6607(9)	0.9789(8)	0.15169(8)	0.086(3)
O23	18f	0.3132(7)	0.9767(7)	0.15362(8)	0.088(3)
O24	18f	0.4455(6)	0.8978(7)	0.16380(6)	0.093(2)

Table 4 ctd. Atomic coordinates and equivalent isotropic displacement parameters ($Å^2$) for extraframework cations and anions in kircherite.

Atom	Wyck.	Occ.	x	y	Z	U(eq)
K1	18f	1	0.21935(14)	0.78244(14)	0.026734(9)	0.0316(2)
Na1	3a	1	0	0	0	0.0620(19)
Na2A	9d	0.616(16)	0	0.49632(18)	0	0.0281(7)
Ca2B	9d	0.384(16)	0	0.49632(18)	0	0.0281(7)
Ca3	6c	1.009(8)	2/3	1/3	0.035016(17)	0.0283(5)
Na4A	18f	0.771(12)	0.4865(2)	0.97775(17)	0.055175(17)	0.0383(6)
Ca4B	18f	0.229(12)	0.4865(2)	0.97775(17)	0.055175(17)	0.0383(6)
Na5A	6c	0.720(14)	0	0	0.06575(15)	0.051(2)
Ca5B	6c	0.280(14)	0	0	0.05922(19)	0.051(2)
Na6A	18f	0.644(9)	0.3399(6)	0.1714(5)	0.08322(4)	0.0451(10)
K6B	18f	0.249(4)	0.4289(6)	0.2173(6)	0.07941(5)	0.0451(10)
Na6B	18f	0.193(8)	0.2762(19)	0.1439(16)	0.08739(14)	0.0451(10)
Na7A	6c	0.05(2)	1/3	2/3	0.08904(2)	0.0354(7)
Ca7B	6c	0.95(2)	1/3	2/3	0.08904(2)	0.0354(7)
Na8A	6c	0.452(15)	2/3	1/3	0.10234(13)	0.055(3)
Na8B	6c	0.08(2)	2/3	1/3	0.1135	0.055(3)
Na8C	6c	0.68(2)	2/3	1/3	0.12063(11)	0.055(3)
K9A	18f	0.236(5)	0.1242(10)	0.2467(9)	0.10791(7)	0.0544(14)
Na9A	18f	0.630(9)	0.1591(7)	0.3183(7)	0.11131(5)	0.0544(14)
Na9B	18f	0.203(7)	0.2035(18)	0.4025(18)	0.11546(13)	0.0544(14)
Na1C	6c	0.53(2)	0	0	0.13014(15)	0.065(4)
Na1D	6c	0.18(3)	0	0	0.1396	0.065(4)
Na1E	6c	0.50(2)	0	0	0.14781(19)	0.065(4)
Na1F	18f	0.23(3)	0.4939(10)	0.9927(7)	0.13870(8)	0.016(3)
K1G	18f	0.411(16)	0.4686(13)	0.930(2)	0.13597(9)	0.117(7)
Na1G	18f	0.367(13)	0.5223	1.0488(18)	0.1413	0.117(7)
Na1K	6c	0.516(17)	1/3	2/3	0.15719(9)	0.044(3)
K1L	18f	0.210(4)	0.2474(9)	0.1287(10)	0.17056(6)	0.0575(16)
Na1L	9d	0.580(7)	1/3	0.1667(9)	1/6	0.0575(16)
Ow25	6*c*	0.94(4)	0	0	0.02844(18)	0.148(10)
S1	6*c*	1	0.3333	0.6667	0.00351(2)	0.0270(3)
O1SA	6*c*	1	0.6667	0.3333	0.01182(7)	0.0530(18)
O1SB	18*f*	1	0.2093(3)	0.6027(5)	0.00861(5)	0.0464(9)
S2	6*c*	1	0.3333	0.6667	0.05032(2)	0.0313(4)
O2SA	6*c*	1	0.3333	0.6667	0.06586(9)	0.0553(8)
O2SB	18*f*	1	0.2101(4)	0.6033(6)	0.04503(5)	0.0553(8)
S3	18*f*	0.307(7)	0.6293(5)	0.2982(5)	0.06703(5)	0.0616(15)
O3SA	18*f*	0.158(11)	0.5436(13)	0.2755(19)	0.07575(14)	0.0553(8)
O3SB	18*f*	0.142(10)	0.6010(19)	0.2033(13)	0.05750(14)	0.0553(8)
S4	18*f*	0.300(6)	-0.005(2)	-0.0256(11)	0.09660(6)	0.088(3)
O4SA	18*f*	0.169(11)	0.0632	-0.0619	0.1048	0.0553(8)
O4SB	18*f*	0.135(10)	-0.0589	-0.1188	0.0872	0.0553(8)
S5	18*f*	0.229(7)	0.3110(8)	0.6776(9)	0.12342(4)	0.0473(17)
O5SA	18*f*	0.151(11)	0.394	0.7873	0.1326	0.0553(8)
O5SB	18*f*	0.119(11)	0.2726	0.7297	0.1137	0.0553(8)
S6	18*f*	0.94(4)	0.7000(8)	0.3668(8)	0.15261(7)	0.060(3)
O6SA	18*f*	0.307(7)	0.7945	0.3943	0.1438	0.0553(8)
O6SB	18*f*	0.158(11)	0.7271	0.4598	0.1613	0.0553(8)

Table 5a. Selected distances of framework cations for kircherite.

Si1—O1^{i}	1.604(4)	Al1—O1	1.722(5)
Si1—O1^{ii}	1.604(4)	Al1—O1^{xii}	1.722(5)
Si1—O1^{iii}	1.619(4)	Al1—O3^{xiii}	1.761(4)
Si1—O1	1.619(4)	Al1—O3^{xiv}	1.761(4)
<Si1—O>	1.612	<Al1—O>	1.742
Si2—O4	1.611(4)	Al2—O7	1.725(4)
Si2—O3	1.599(4)	Al2—O5	1.756(5)
Si2—O5^{v}	1.590(5)	Al2—O4^{v}	1.717(4)
Si2—O6^{vi}	1.591(4)	Al2—O2	1.724(4)
<Si2—O>	1.598	<Al2—O>	1.731
Si3—O10^{i}	1.616(4)	Al3—O6^{xv}	1.706(5)
Si3—O9	1.623(5)	Al3—O8^{xv}	1.732(5)
Si3—O8^{i}	1.590(5)	Al3—O9	1.735(4)
Si3—O7	1.615(4)	Al3—O11	1.735(5)
<Si3—O>	1.611	<Al3—O>	1.727
Si4—O11	1.586(5)	Al4—O15^{x}	1.705(5)
Si4—O12^{viii}	1.601(6)	Al4—O13^{viii}	1.744(5)
Si4—O14	1.592(5)	Al4—O12	1.708(6)
Si4—O13	1.580(5)	Al4—O10	1.733(5)
<Si4—O>	1.590	<Al4—O>	1.723
Si5—O18	1.581(5)	Al5—O14	1.731(5)
Si5—O17	1.609(7)	Al5—O16	1.705(7)
Si5—O16	1.597(7)	Al5—O17^{xvi}	1.680(7)
Si5—O15	1.602(5)	Al5—O19	1.724(6)
<Si5—O>	1.597	<Al5—O>	1.710
Si6—O19	1.579(6)	Al6—O21	1.716(7)
Si6—O22^{viii}	1.577(6)	Al6—O20^{iv}	1.715(7)
Si6—O21	1.554(7)	Al6—O23^{iii}	1.689(6)
Si6—O20	1.565(6)	Al6—O18	1.695(6)
<Si6—O>	1.569	<Al6—O>	1.704
Si7—O24	1.584(7)	Al7—O22	1.710(6)
Si7—O24^{ix}	1.584(7)	Al7—O22^{xi}	1.710(6)
Si7—O23	1.571(5)	Al7—O24^{xi}	1.673(7)
Si7—O23^{ix}	1.572(5)	Al7—O24	1.673(7)
<Si7—O>	1.578	<Al7—O>	1.692

Symmetry codes:
(i) x-y, -y, -z; (ii) 1+x-y, 1-y, -z; (iii) x, -1+y, z; (iv) -x+y, -x, z;
(v) 1-y, x-y, z; (vi) 1+x, y, z; (vii) 2-y, 1+x-y, z; (viii) -x+y, 1-x, z;
(ix) 0.66667-x, 0.33333-x+y, 0.33333-z; (x) x, 1+y, z;
(xi) -0.33333+y, 0.33333+x, 0.33333-z; (xii) -x, -x+y, -z;
(xiii) 1-x, 1-x+y, -z; (xiv) -1+x, y, z; (xv) 1-y, 1+x-y, z; (xvi) 1-x+y, 1-x, z

Table 5b. Selected distances of extra-framework cations sites for kircherite.

K1-O1SB^{VIII}	2.788(6)	Na1-O1^{XVII}	2.648(3)	Na2A-O3XIV	2.471(5)	Ca3-O1SA	2.209(7)
K1-O2SB^{VIII}	2.800(7)	Na1-O1^{XV}	2.648(3)	Na2A-O3XIII	2.471(5)	Ca3-O4^{XVI}	2.447(3)
K1-O6	2.803(5)	Na1-O1^{II}	2.648(3)	Na2A-O1SB	2.474(4)	Ca3-O4^{V}	2.447(3)
K1-O1SB	2.839(5)	Na1-O1^{XVIII}	2.648(3)	Na2A-O1SBXII	2.474(4)	Ca3-O4	2.447(3)
K1-O7^{X}	2.840(5)	Na1-O1^{XIX}	2.648(3)	Na2A-O2XX	2.498(4)	Ca3-O3SB^{V}	2.586(14)
K1-O2SB	2.845(7)	Na1-O1^{I}	2.648(3)	Na2A-O2XXI	2.499(4)	Ca3-O3SB	2.586(14)
K1-O2^{X}	2.902(5)	Na1-Ow25^{XX}	2.709(17)	Na2A-O5XXI	2.965(3)	Ca3-O3SB^{XVI}	2.586(14)
K1-O3^{XIV}	2.958(5)	Na1-Ow25	2.709(17)	Na2A-O5XX	2.965(3)	Ca3-O5	2.885(3)
K1-O1	3.216(3)	<Na1-O>	2.663	<Na2A-O>	2.602	Ca3-O5^{V}	2.885(3)
<K1-O>	2.888					Ca3-O5^{XVI}	2.885(3)
		Na5A-O4SB^{XXI}	2.435(12)	Ca5B-O8^{XVIII}	2.429(4)	<Ca3-O>	2.596
Na4A-O2SB^{VIII}	2.307(5)	Na5A-O4SB^{IV}	2.435(12)	Ca5B-O8^{I}	2.429(4)		
Na4A-O11XV	2.498(7)	Na5A-O4SB	2.435(12)	Ca5B-O8^{XV}	2.429(4)	Na6A-O3SA	2.381(16)
Na4A-O10	2.504(6)	Na5A-O8X^{VII}I	2.587(6)	Ca5B-O9^{IV}	2.831(3)	Na6A-O14	2.422(8)
Na4A-O3SBX	2.525(15)	Na5A-O8I	2.587(6)	Ca5B-O9	2.831(3)	Na6A-O9	2.465(4)
Na4A-O6VIII	2.593(6)	Na5A-O8^{XV}	2.587(6)	Ca5B-O9^{XXI}	2.831(3)	Na6A-O4SB^{XXI}	2.495(7)
Na4A-O7X	2.597(5)	Na5A-O9^{IV}	2.895(5)	Ca5B-Ow25	2.93(3)	Na6A-O15	2.512(9)
Na4A-O5X	2.672(3)	Na5A-O9	2.895(5)	Ca5B-O4S^{BXXI}	2.976(16)	Na6A-O10^{I}	2.675(7)
Na4A-O12	2.914(4)	Na5A-O9^{XXI}	2.895(5)	Ca5B-O4SB^{IV}	2.976(16)	Na6A-O11	2.759(8)
<Na4A-O>	2.576	<Na5A-O>	2.639	Ca5B-O4SB	2.976(16)	Na6A-O16	2.888(6)
		Na5A-Ca5B	0.622(15)	<Ca5B-O>	2.801	<Na6A-O>	2.575
Na6B-O14	2.336(17)			Na6A-Na6B	0.816(18)		
Na6B-O15	2.501(18)	K6B-O9	2.730(6)	Na6A-K6B	1.057(8)	Na7A-O2SA	2.207(9)
Na6B-O9	2.681(13)	K6B-O14	2.757(9)	K6B-Na6B	1.87(2)	Na7A-O12^{XV}	2.542(4)
Na6B-O16	2.952(14)	K6B-O10^{I}	2.776(8)			Na7A-O12	2.542(4)
Na6B-O11	2.972(18)	K6B-O11	2.826(9)	Na8C-O16V	2.583(7)	Na7A-O12^{VIII}	2.542(4)
Na6B-O10^{I}	2.986(18)	K6B-O15	2.880(11)	Na8C-O16	2.583(7)	Na7A-O13^{VIII}	2.686(4)
<Na6B-O>	2.738	K6B-O16	2.979(6)	Na8C-O16XVI	2.583(7)	Na7A-O13^{XV}	2.686(4)
		K6B-O3SB^{XVI}	3.10(2)	Na8C-O6SA	2.628(9)	Na7A-O13	2.686(4)
Na8A-O16^{V}	2.523(6)	<K6B-O>	2.864	Na8C-O6SAXVI	2.628(9)	Na7A-O5SB	2.7255(17)
Na8A-O16^{XVI}	2.523(6)			Na8C-O6SAV	2.628(9)	Na7A-O5SB^{VIII}	2.7255(17)
Na8A-O16	2.523(6)	Na8B-O16^{V}	2.414(5)	Na8C-O17	2.868(6)	Na7A-O5SB^{XV}	2.7255(17)
Na8A-O3SA	2.881(18)	Na8B-O16^{XVI}	2.414(5)	Na8C-O17V	2.868(6)	<Na7A-O>	2.607
Na8A-O3SA^{V}	2.881(18)	Na8B-O16	2.414(6)	Na8C-O17XVI	2.868(6)		
Na8A-O3SA^{XVI}	2.881(18)	Na8B-O17^{V}	2.828(6)	<Na8C-O>	2.693	Na8A-Na8B	1.063(12)
<Na8A-O>	2.702	Na8B-O17	2.828(6)			Na8A-Na8C	1.742(18)
		Na8B-O17^{XVI}	2.828(6)	Na9B-O19	2.49(2)	Na8B-Na8C	0.679(11)
Na9A-O4SA^{XXI}	2.242(8)	<Na8B-O>	2.621	Na9B-O13	2.613(12)		
Na9A-O19	2.465(10)			Na9B-O18^{XXI}	2.66(2)	Na1K-Na1KXI	1.806(17)
Na9A-O13	2.511(5)	K9A-O19	2.727(13)	Na9B-O20	2.894(15)	Na1K-O24	2.654(7)
Na9A-O5SB^{XV}	2.515(8)	K9A-O15^{XXI}	2.731(13)	<Na9B-O>	2.664	Na1K-O24XV	2.654(7)
Na9A-O18^{XXI}	2.624(12)	K9A-O13	2.745(8)	K9A-Na9A	0.861(9)	Na1K-O24VIII	2.654(7)
Na9A-O15^{XXI}	2.681(10)	K9A-O14	2.760(12)	K9A-Na9B	1.88(2)	Na1K-O5SA^{XV}	2.701(7)
Na9A-O20	2.695(7)	K9A-O20	2.807(8)	Na9A-Na9B	1.019(18)	Na1K-O5SA	2.701(7)
Na9A-O14	2.741(9)	K9A-O18^{XXI}	2.909(15)			Na1K-O5SA^{VIII}	2.701(7)
<Na9A-O>	2.559	K9A-O4SB^{XXI}	3.085(10)	Na1E-O20^{XXI}	2.670(10)	Na1K-O24XI	2.834(9)
		<K9A-O>	2.823	Na1E-O20^{IV}	2.670(10)	Na1K-O24^{XXV}	2.834(9)
Na1C-O20	2.563(7)			Na1E-O20	2.670(10)	Na1K-O24^{IX}	2.834(9)
Na1C-O20^{XXI}	2.563(7)	Na1D-O20^{XXI}	2.483(7)	Na1E-O6SB^{XXIII}	2.703(15)	<Na1K-O>	2.730
Na1C-O20^{IV}	2.563(7)	Na1D-O20	2.483(7)	Na1E-O6SB^{XXIV}	2.703(15)		
Na1C-O4SA^{IV}	2.788(13)	Na1D-O20^{IV}	2.483(7)	Na1E-O6SB^{IX}	2.703(15)	K1L-O21	2.647(9)
Na1C-O4SA	2.788(13)	Na1D-O21^{IV}	2.697(7)	Na1E-O21^{IV}	2.722(7)	K1L-O22XXV	2.735(14)
Na1C-O4SA^{XXI}	2.788(13)	Na1D-O21	2.697(7)	Na1E-O21	2.722(7)	K1L-O21IX	2.760(11)
Na1C-O21^{IV}	2.938(10)	Na1D-O21^{XXI}	2.697(7)	Na1E-O21^{XXI}	2.722(7)	K1L-O23XVI	2.798(13)
Na1C-O21	2.938(10)	<Na1D-O>	2.590	<Na1E-O>	2.698	K1L-S6XXIV	2.967(15)
Na1C-O21^{XXI}	2.938(10)	Na1D-Na1E	0.782(18)			K1L-O23I	2.968(14)
<Na1C-O>	2.763	Na1C-Na1D	0.901(14)	Na1G-O17X	2.504(5)	K1L-O22VIII	2.991(15)
		Na1C-Na1E	1.68(3)	Na1G-O22	2.563(19)	K1L-O6SAXXIV	2.992(10)
Na1F-O5SA	2.363(8)			Na1G-O23	2.644(10)	<K1L-O>	2.857
Na1F-O6SA^{XXII}	2.423(8)	K1G-O17^{X}	2.588(12)	Na1G-O24	2.724(15)		
Na1F-O17^{X}	2.435(9)	K1G-O24	2.676(9)	Na1G-O18X	2.737(12)	Na1L-O6SB^{V}	2.3629(2)
Na1F-O22	2.561(15)	K1G-O22	2.684(17)	Na1G-O19XV	2.935(15)	Na1L-O6SB^{XXIII}	2.3630(2)
Na1F-O18^{X}	2.597(15)	K1G-O18^{X}	2.718(13)	<Na1G-O>	2.685	Na1L-O21	2.502(7)
Na1F-O24	2.614(10)	K1G-O19^{XV}	2.738(12)			Na1L-O21^{IX}	2.503(7)
Na1F-O23	2.646(15)	K1G-O23	2.898(15)			Na1L-O23^{I}	2.638(14)
Na1F-O19^{XV}	2.784(15)	<K1G-O>	2.717			Na1L-O23^{XVI}	2.638(14)
<Na1F-O>	2.553	Na1F-Na1G	0.673(19)			Na1L-O22^{VIII}	2.729(14)
		Na1F-K1G	0.75(2)	K1L-Na1L	1.030(10)	Na1L-O22^{XXV}	2.729(14)
		K1G-Na1G	1.42(3)	K1L-K1LIX	2.06(2)	<Na1L-O>	2.558

Symmetry transformations used to generate equivalent atoms:
(I) x,y-1,z; (II) x-y+1,-y+1,-z; (III) x-y,-y,-z; (IV) -x+y,-x,z; (V) -y+1,x-y,z; (VI) x+1,y,z; (VII) -y+2,x-y+1,z; (VIII) -x+y,-x+1,z; (IX) -x+2/3,-x+y+1/3,-z+1/3; (X) x,y+1,z; (XI) y-1/3,x+1/3,-z+1/3; (XII) -x,-x+y,-z; (XIII) -x+1,-x+y+1,-z; (XIV) x-1,y,z; (XV) -y+1,x-y+1,z; (XVI) -x+y+1,-x+1,z; (XVII) -x,-x+y-1,-z; (XVIII) -x+y-1,-x,z; (XIX) y-1,x,-z ; (XX) y,x,-z ; (XXI) -y,x-y,z (XXII) -x+y+1,-x+2,z; (XXIII) y-1/3,x-2/3,-z+1/3; (XXIV) x-y-1/3,-y+1/3,-z+1/3; (XXV) x-y+2/3,-y+4/3,-z+1/3; (XXVI) -x+2/3,-x+y-2/3,-z+1/3; (XXVII) -x+2/3,-x+y+4/3,-z+1/3; (XXVIII) y+2/3,x+1/3,-z+1/3; (XXIX) x-y+2/3,-y+1/3,-z+1/3

Table 5c. Selected distances of extra-framework anionic groups for kircherite.

S1-O1SA^{XX}	1.461(7)	S2-O2SB	1.464(5)	S3-O3SA	1.293(16)
S1-O1SB^{VIII}	1.466(4)	S2-O2SB^{VIII}	1.464(5)	S3-O3SB	1.416(16)
S1-O1SB	1.466(4)	S2-O2SB^{XV}	1.464(5)	S3-O3SA^{V}	1.679(16)
S1-O1SB^{XV}	1.466(4)	S2-O2SA	1.481(8)	S3-O3SB^{XV}I	1.755(16)
<S1-O>	1.465	<S2-O>	1.468	S3-S3^{V}	0.809(9)
S4-O4SB	1.375(11)	S5-O5SB	1.371(4)	S6-O6SB	1.351(9)
S4-O4SA	1.42(2)	S5-O5SA^{XV}	1.430(9)	S6-O6SA	1.370(9)
S4-O4SA^{IV}	1.58(2)	S5-O5SA	1.547(9)	S6-O6SB^{XVI}	1.684(10)
S4-O4SB^{XXI}	1.67(2)	S5-O5SB^{XV}	1.798(8)	S6-O6SA^{V}	1.698(10)
S4-S4^{XXI}	0.52(2)	S5-S5^{VIII}	0.657(8)	S6-S6^{V}	0.745(14)

Symmetry transformations used to generate equivalent atoms:
(IV) -x+y,-x,z; (V) -y+1,x-y,z; (VIII) -x+y,-x+1,z; (X) x,y+1,z; (XI) y-1/3,x+1/3,-z+1/3;
(XV) -y+1,x-y+1,z; (XVI) -x+y+1,-x+1,z; ; (XX) y,x,-z ; (XXI) -y,x-y,z

Table 6. Cation site assignments on the basis of observed site scattering and geometries of the sites reported in Table 5 for kircherite

atom	Site multiplicity	Site occupancy factor	Site scattering (eps)*	Cation population (apfu)**
K1	18*f*	1.000	19	18 K
Na1	3*a*	1.000	11.0	3 Na
Na2A	9*d*	0.616(16)	14.5	5.54 Na + 3.46 Ca
Ca2B	9*d*	0.384(16)		
Ca3	6*c*	1.009(8)	20.2	6 Ca
Na4A	18*f*	0.771(12)	13.1	13.88 Na + 4.12 Ca
Ca4B	18*f*	0.229(12)		
Na5A	6*c*	0.720(14)	13.5	4.32 Na + 1.68 Ca
Ca5B	6*c*	0.280(14)		
Na6A	18*f*	0.644(9)	13.9	11.60 Na + 4.48 K +1.91 Ca
K6B	18*f*	0.249(4)		
Na6B	18*f*	0.193(8)		
Na7A	6*c*	0.05(2)	19.6	5.70 Ca + 0.30 Na
Ca7B	6*c*	0.95(2)		
Na8A	6*c*	0.452(15)	13.3	4.46 Na + 1.55 Ca
Na8B	6*c*	0.08(2)		
Na8C	6*c*	0.68(2)		
K9A	18*f*	0.236(5)	13.6	12.24 Na + 4.25 K +1.52 Ca
Na9A	18*f*	0.630(9)		
Na9B	18*f*	0.203(7)		
Na1C	6*c*	0.53(2)	13.3	4.46 Na + 1.54 Ca
Na1D	6*c*	0.18(3)		
Na1E	6*c*	0.50(2)		
Na1F	18*f*	0.23(3)	14.4	10.71 Na + 5.02 K +2.28 Ca
K1G	18*f*	0.411(16)		
Na1G	18*f*	0.367(13)		
Na1K	6*c*	0.516(17)	5.7	2.88 Na+ 0.12 Ca
K1L	18*f*	0.210(4)	4.0	3.78 K
Na1L	9*d*	0.580(7)	6.4	5.22 Na
Total extra framework cations (XRD)				78.62 Na + 35.53 K + 29.86 Ca
Total extra framework cations (EMPA)				89.09 Na + 18.85 K + 31.63 Ca
Ow25	6*c*	0.94(4)	45.1	5.64 H_2O
S1	6*c*	1	96	6 S
S2	6*c*	1	96	6 S
S3	18*f*	0.333	96	5.04 S+0.84 Cl+0.02 F***
S4	18*f*	0.300(6)	88.4	4.80 S+0.40 Cl+0.46 H_2O+0.12 F
S5	18*f*	0.229(7)	86.4	4.71 S+0.34 Cl+0.45 H_2O+0.17 F
S6	18*f*	0.94(4)	66.0	3.51 S+0.35 Cl+0.35 H_2O+0.13 F

* eps = electrons per site, **apfu (atoms per formula unit); *** We opted to assign Cl, F and excess H2O over the amount in Ow25 disordered over S3, S4,S5 and S6 because splitting off axis did not allowed to distinguish the different species. The sum < 6 apfu per site is to ascribe to the difficulty on modelling the disordering.

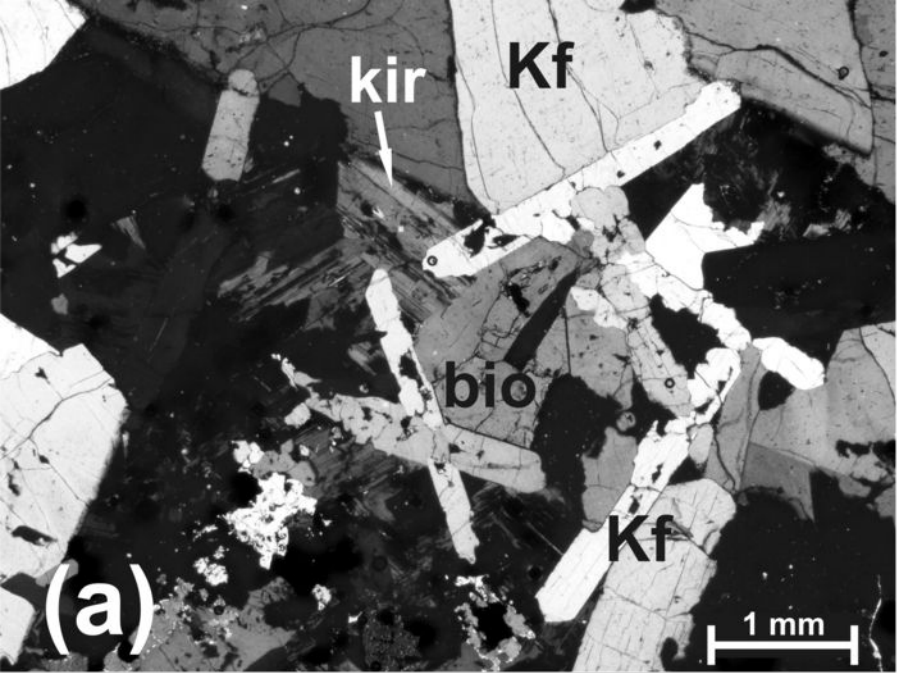

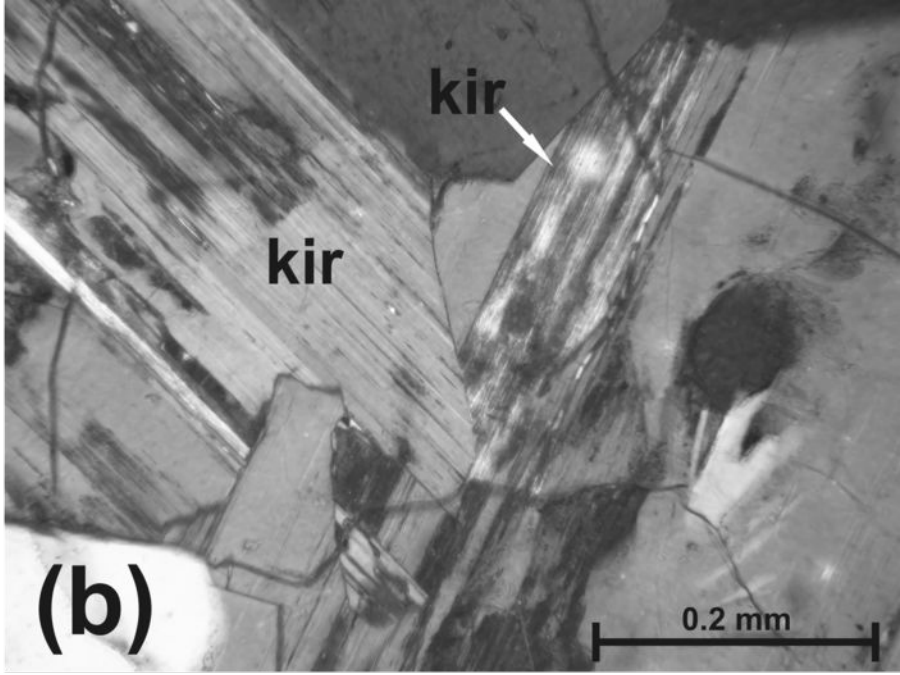

Figure 1

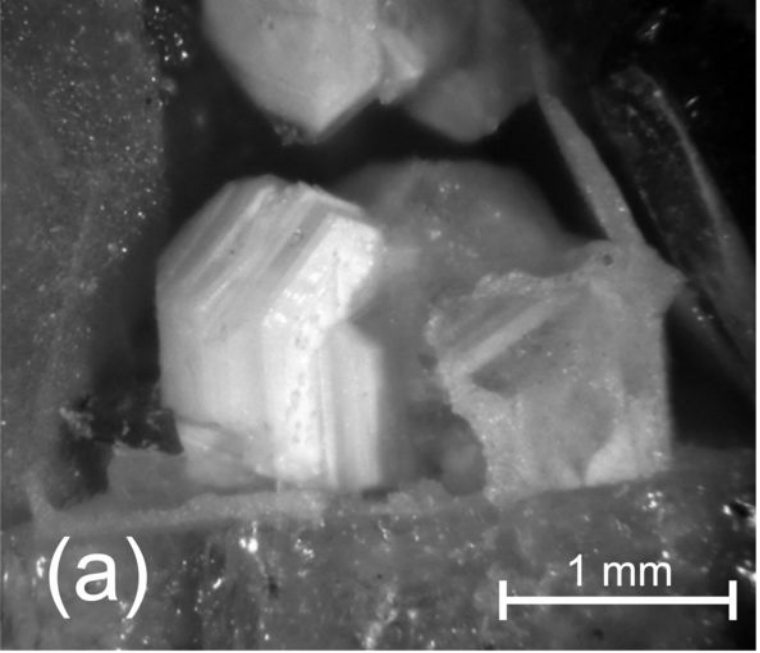

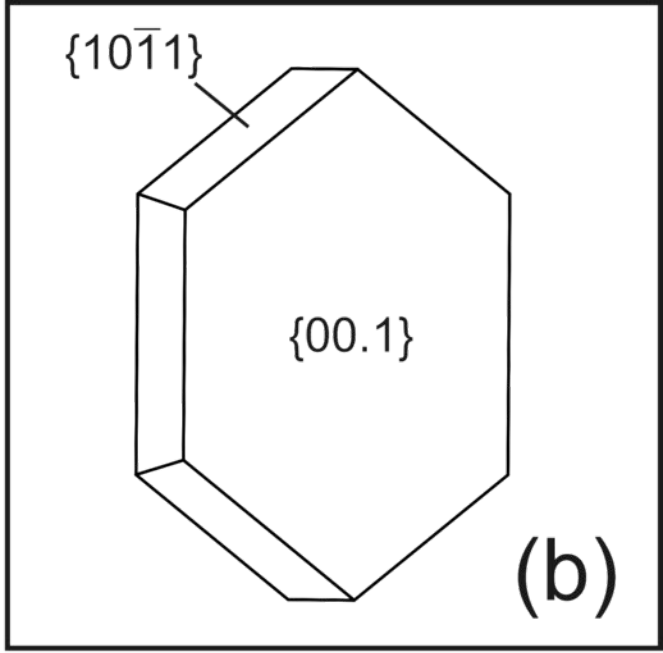

Figure 2 first revision

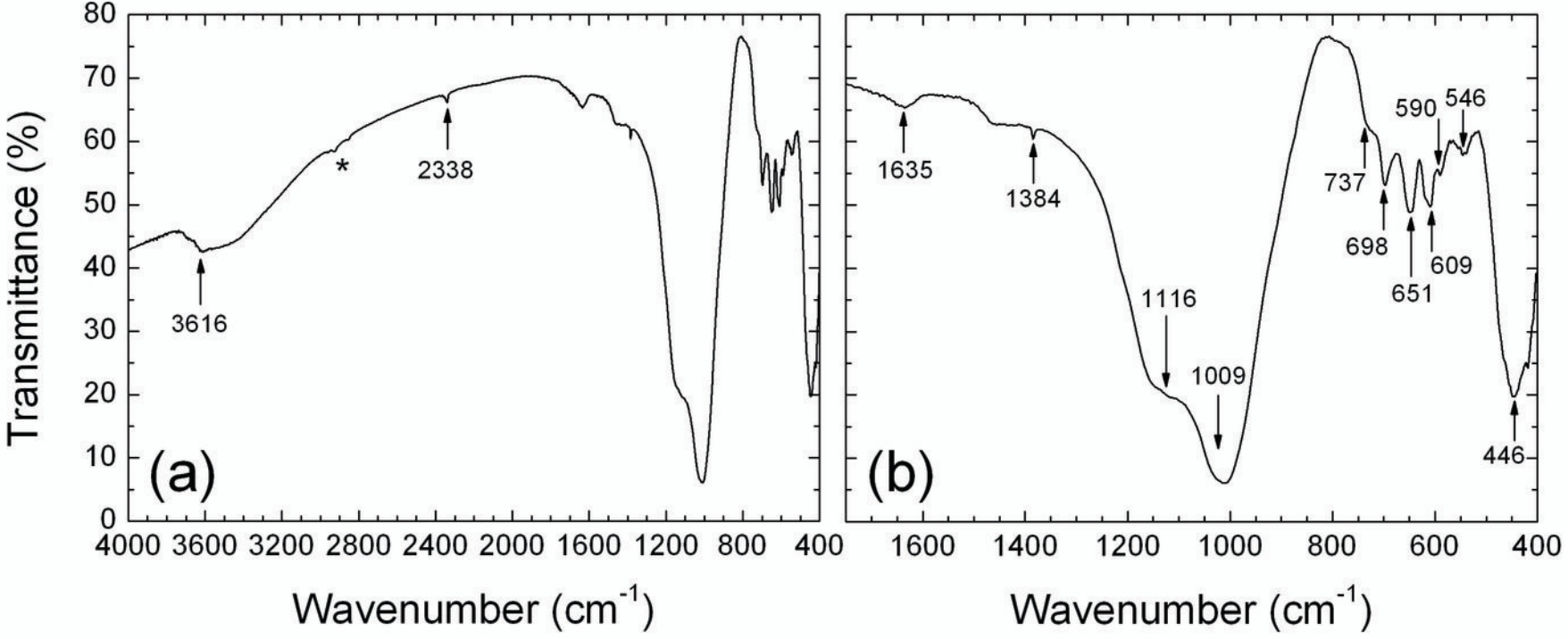
Transmittance (%)
80
70
60
50
40
30
20
10
0
4000 3600 3200 2800 2400 2000 1600 1200 800 400
Wavenumber (cm-1)
(a)
3616
*
2338
1600 1400 1200 1000 800 600 400
Wavenumber (cm-1)
(b)
1635
1384
1116
1009
737
590
546
698
651
609
446

Figure 3

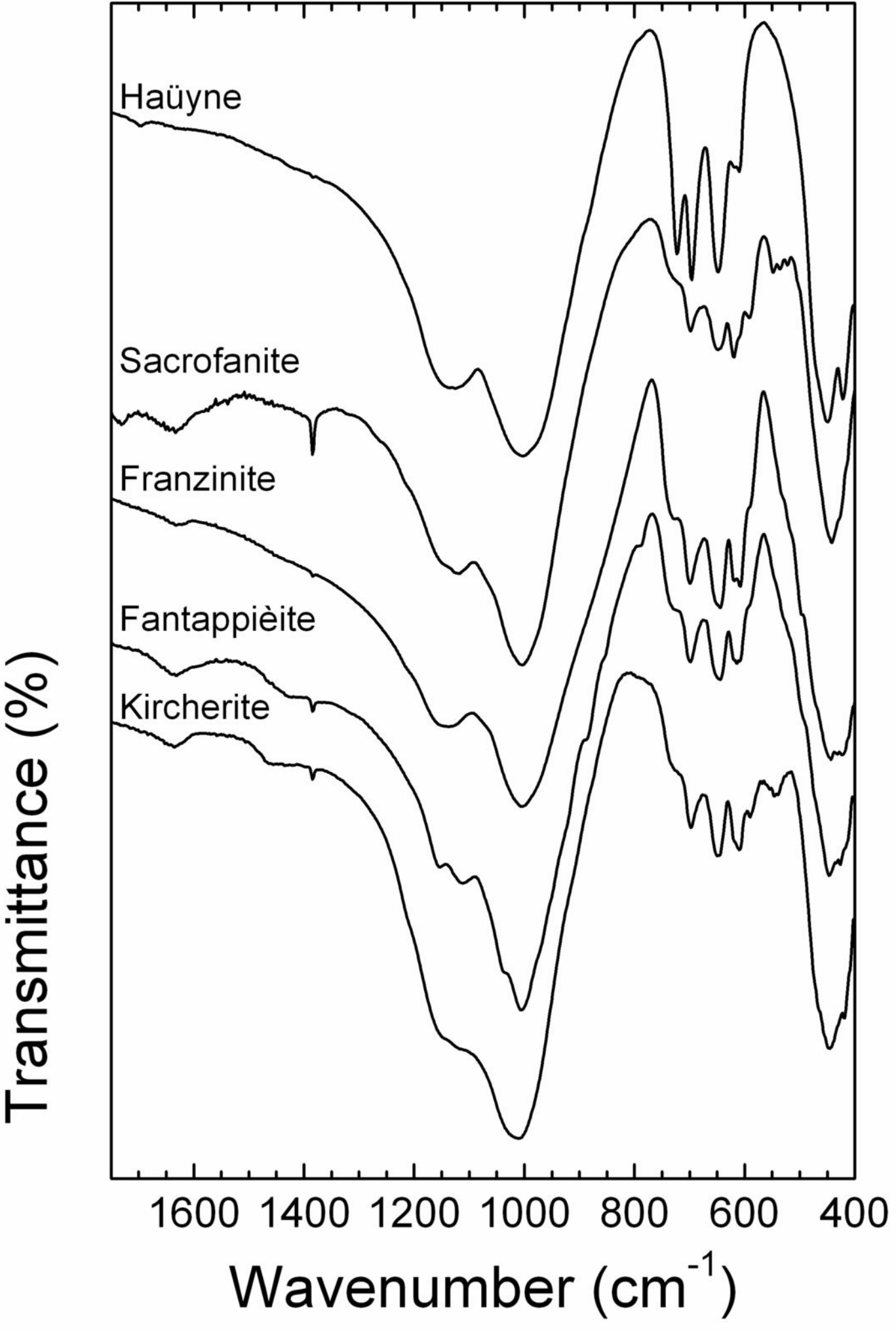
Haüyne
Sacrofanite
Franzinite
Fantappièite
Kircherite
Transmittance (%)
1600 1400 1200 1000 800 600 400
Wavenumber (cm-1)

Figure 4

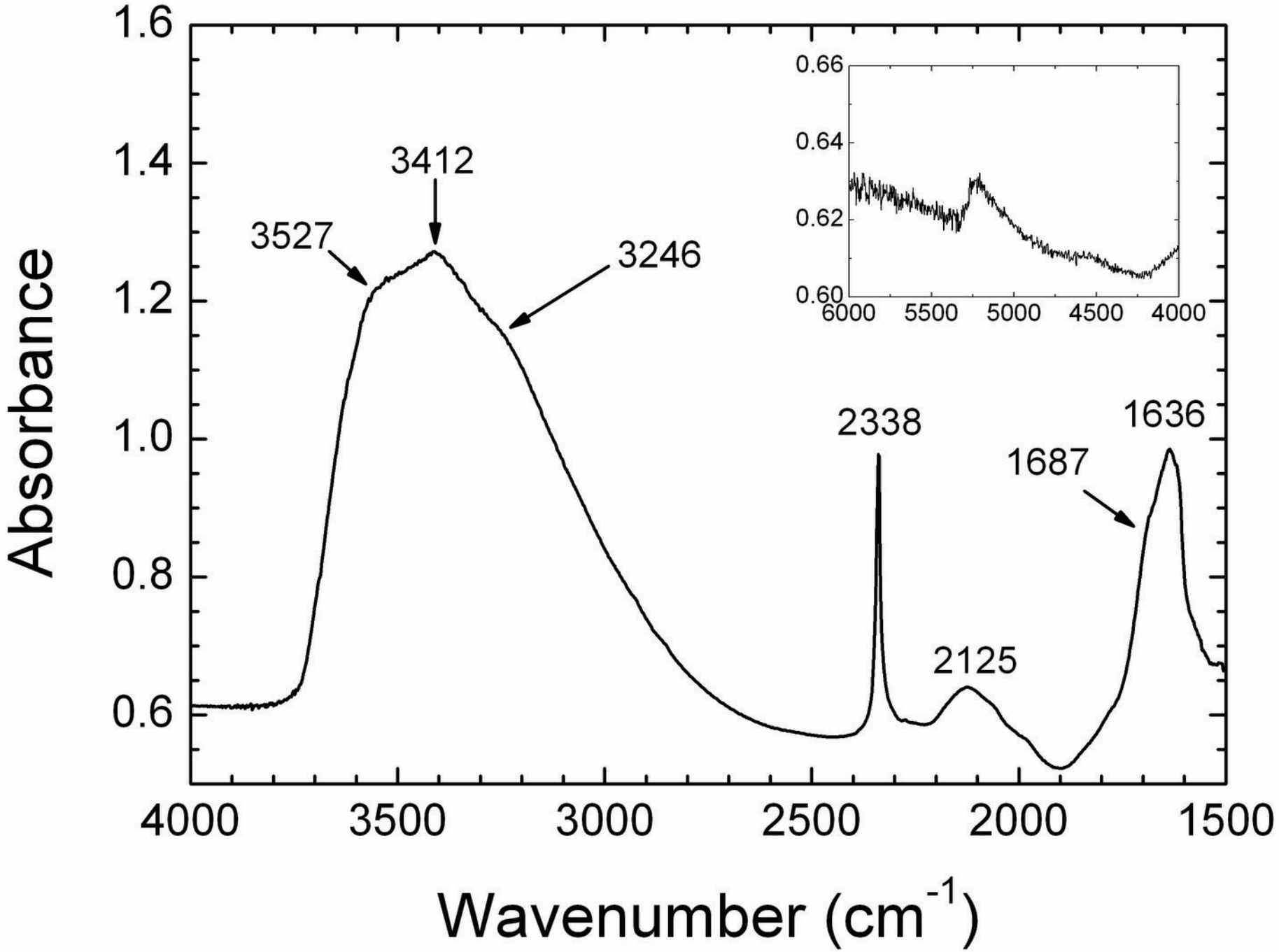
Absorbance
Wavenumber (cm-1)
3527
3412
3246
2338
2125
1687
1636
1.6
1.4
1.2
1.0
0.8
0.6
4000
3500
3000
2500
2000
1500
0.66
0.64
0.62
0.60
6000
5500
5000
4500
4000

Figure 5

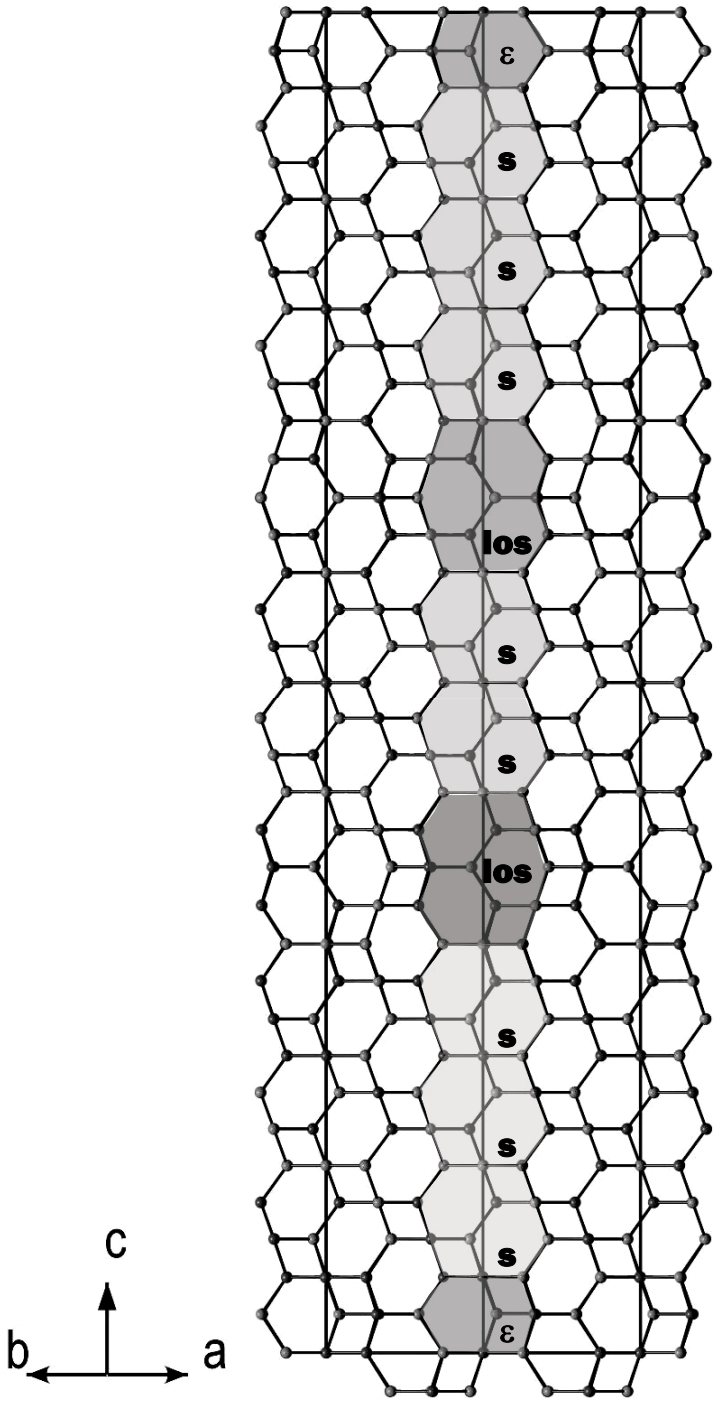

Figure 6